Polymer(Korea), Vol. 40, No. 2, pp. 209-215 (2016)
http://dx.doi.org/10.7317/pk.2016.40.2.209
ISSN 0379-153X(Print)
ISSN 2234-8077(Online)

생체공학적 고분자 렌즈 시스템의 제조와 분석

Xuan Yin Wang, Dan Liang†, Feng Tang, and Jia Wei Du
The State Key Laboratory of Fluid Power and Mechatronic Systems, Zhejiang University
(2015년 9월 20일 접수, 2015년 12월 11일 수정, 2015년 12월 12일 채택)

Fabrication and Analyses of Bionic Polymer Lens System

Xuan Yin Wang, Dan Liang†, Feng Tang, and Jia Wei Du
The State Key Laboratory of Fluid Power and Mechatronic Systems, Zhejiang University, *Hangzhou* 310027, *P. R. China*
(Received September 20, 2015; Revised December 11, 2015; Accepted December 12, 2015)

Abstract: In this paper, we design and fabricate a bionic solid tunable lens which is mainly made of polymer materials. The lens focal length can be changed flexibly by pressing the lens surface to alter the curvature radius. A detailed description of the lens structure, materials and fabrication process is presented. The lens mechanical properties and deformation process are simulated and analyzed using Ansys software. A precise experimental device based on a stepping motor is fabricated to measure and analyze the relationship between the displacement load and focal length. The lens focal length can be reversibly changed from 31.8 to 14.1 mm under 1 mm variation of displacement load. This paper offers a feasible way for the design, fabrication, and actuation of the solid tunable lens, which can be used in various machine vision apparatus.

Keywords: tunable lens, polymer material, deformation and stress analyses, actuation device.

Introduction

Nowadays, the demand for portable imaging devices is growing faster and faster with the advances in technology. As the core component of visual imaging apparatus, the zoom lens system attracts a great deal of attention. How to make the zoom system more compact and stable with less power consumption and higher image quality is one of the key issues. Conventional zoom system consists of multiple rigid lenses, and adjusts the focal length by changing the position of different lenses with gears and electrical motor driver. This kind of zoom system needs to move the lenses back and forth to adjust the focus which limits the miniaturization of the system and complicates the mechanical transmission structure. Therefore, it is of great significance to consider the zoom issues from other perspectives and study new tunable lenses to promote the development and application of the zoom technology.

The human eyes focus on desirable objects by squeezing the crystalline lens through ciliary muscle, so that the targets of different distances can image on the retina clearly. Inspired by the human focusing system, a variety of tunable lenses for the zoom system have been designed and studied in recent years, which offers a feasible way to substitute the conventional lens for its miniature size and favorable controllability. The tunable lens changes either the lens curvature radius or the refractive index of the optical medium to adjust the focal length. The former case generally alters the curvature in one of two ways: compressing the elastic membrane encapsulating optical liquid,[1-9] or applying electro-wetting principles to change the curvature of the meniscus between two immiscible liquids.[10,11] The latter case usually makes use of specific liquid crystal materials and changes the focal length by controlling the applied voltage.[12,13] Among the elastic membrane lenses, various kinds of actuation mechanisms are introduced to drive the deformation, including micro electric motor, transparent dielectric elastomer actuator (DEAs), ionic polymer metal composite (IPMC) device and micropump. However, there are various problems facing the tunable lenses mentioned above. The liquid tunable lens is susceptible to temperature alteration and external vibration, and usually has low optical axis stability, which leads to distortion and spherical aberration. The lens based on electro-wetting usually requires a relatively high

†To whom correspondence should be addressed.
E-mail: ldldld7777@163.com

voltage and constructing a large aperture electro-wetting lens is challenging. The tunable lens made from liquid crystal materials generally has inherent optical limitations such as polarization effects and relatively slow response time.

Instead of using liquid as optical medium for the tunable lens, adopting solid state material with good elasticity can be more robust to the fluctuations in temperature, vibration, and motion. Several preliminary research about solid tunable lens has been published. A humanoid focusing mechanism which consisted of parylene nanofibers and soft polymer lens is presented and demonstrated.[14] A solid-state tunable lens based on shape changes in an elastomeric membrane driven by compression of a polymer gel reservoir is described.[15] However, there is much systematic work about the optimization of lens structure, fabrication method, actuation and deformation analysis to be done to further understanding the characteristic of the solid tunable lens and improve the optical performance, stability and controllability.

This paper presents the design, fabrication and property analyses of a solid tunable lens made of polymer materials. The lens focal length is changed along with the variation of its curvature when exerting pressure onto the surface. A detailed description of the lens structure, materials and fabrication process is presented. The lens mechanical properties and deformation process are analyzed through Ansys software. A precise experimental device based on stepping motor is fabricated, and the relationship between the displacement load and focal length is analyzed. Additionally, images captured through the lens under different displacements are presented, and the lens optical property is discussed.

Materials and Methods

The crystalline lens of the human eye is made of soft tissues which are prone to deforming when subjected to the extrusion. The focus of the human eye can be flexibly adjusted through the deformation of the crystalline lens. Inspired by the structure and focusing process of the human eye, this paper presents a solid tunable lens using polymer materials which has high transmittance and refractive index. Besides, a precise actuator is fabricated to imitate the function of the ciliary muscle, which can compress the lens surface to alter the focal length reversibly and precisely. The solid tunable lens (Figure 1) mainly consists of four parts: ethylene butylene-styrene triblock copolymer (SEBS) thin film, poly(dimethyl siloxane) (PDMS) lens, poly(methyl methacrylate) (PMMA) lens and high-density polyethylene (HDPE) gasket. The retaining ring is used to squeeze the surface of the SEBS film to make the PDMS lens deform outward, thus changing the lens focus.

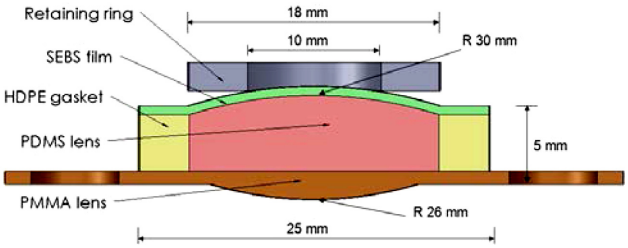

Figure 1. Tunable-focus system.

The SEBS film is made from the ethylene butylene-styrene triblock copolymer material (Kraton G1567 Series SEBS), which has a high refractive index, good optical properties and superior resiliency characteristics. Its dissolution temperature is 150 °C, and decomposition temperature is 270 °C. To fabricate the SEBS film, we design a set of metal molds and fix two glass lenses into the groove of the molds. Then, the SEBS granules are placed between the glass lenses to get molded through hot (under 165 °C, 15 MPa for 10 min) and cold (under room temperature, 15 MPa for 5 min) press molding processes sequentially. After removing the metal molds, the SEBS film is cut into designed diameter. The PMMA lens is made of poly(methyl methacrylate) material (LG IF850),[16,17] which has a high transmittance (approximately 92%) and refractive index (1.41). The HDPE gasket is made of high-density polyethylene,[18] and it has two main functions. One is to connect the PMMA lens and SEBS film to ensure that the shape of the lens peripheral part keeps unchanged when compressed by the retaining ring. The other is to construct a specific cavern together with the PMMA lens and SEBS film to inject the PDMS material. The fabrication process of the HDPE gasket and PMMA lens is the same to SEBS film, using sequential hot and cold pressing process.

Poly(dimethyl siloxane) (PDMS, DOW Corning Sylgard l84) is usually made of pre-polymer and curing agent,[19-21] and the measured refractive index is 1.49. With the less ratio of the curing agent, the PDMS elastomer would become much softer. If the concentration of the curing agent is greater than 10%, the PDMS elastomer becomes rather hard. Taking account of the specific application of the tunable lens, the softer material is more suitable. Thus, we mix the PDMS pre-polymer and curing agent at a ratio of 20:1 by weight. The compound PDMS liquid is degassed by a vacuum pump to make sure its uniformity and transparency.

Figure 2. Manufactured solid tunable lens.

To assemble the designed tunable lens, the PMMA lens, HDPE gasket and SEBS film are firstly bonded by sticky adhesive (Loctite 496). Then, we inject the PDMS mixture into the cavern made up by the lens different parts mentioned above. Meanwhile, the air in the cavern is extracted by a microsyringe. After the injecting procedure, we put the whole compound lens in a thermostatic oven under the temperature of 80 °C for 20 min, and get the solid state lens finally. The initial shape of the PDMS lens without pressure is shown in Figure 1. The overall shape of the solid tunable lens is shown in Figure 2.

Simulation Analyses of the Lens Stress and Deformation

In order to verify the reliability of the structural strength and analyze the lens deformation characteristics, we use the finite element software Ansys to simulate the state of the lens when extruded under different displacement loads. Using finite element analysis software is usually an effective way to verify and simulate the lens deformation. During the extrusion process, the SEBS film is clung to the PDMS lens all the time, so we can consider that their surface deformations are same among the entire process. The PMMA lens is fixed, and the alteration of the lens focus is mainly achieved by varying the curvatures of the SEBS film and PDMS lens.

During the process of modeling and simulation analyses, the tunable-focus system is divided into two parts: tunable-focus part (including aluminum compression ring, SEBS film, PDMS lens and HDPE gasket), and the fixed part (the PMMA lens). Considering the analysis features of the Ansys software, we select the elastomer binomial Mooney-Rivlin theoretical model as the material model of SEBS film and PDMS lens, and selected plane 182 as the unit type. Because the data of modeling the three-dimensional solid is usually very large, we

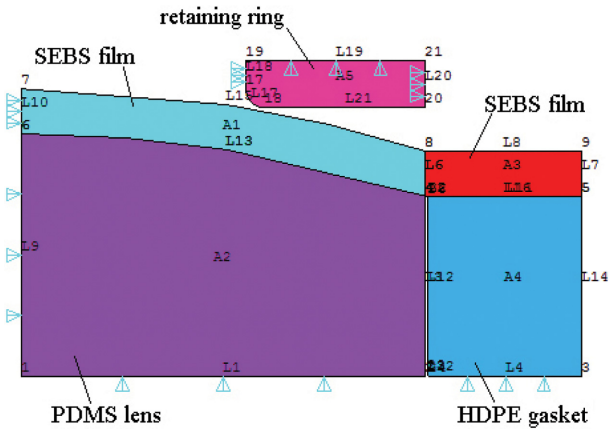

Figure 3. Boundary conditions.

establish a 2D plane model and consider the rotational symmetry of the structure. Figure 3 shows the boundary conditions.

The contact relation between the bottom edge of the retaining ring and the surface of the tunable lens is defined as a line-line contact. The maximum working stroke of the actuator is designed as 1 mm, and the simulation process is divided into four stages by stroke: 0.25, 0.5, 0.75 and 1 mm. The corresponding strain curves of the four stages are shown in Figure 4. It's easy to find that the maximum deformations of the SEBS film along the optical axis direction are as follows: 0.1819, 0.4268, 0.6703 and 1.186 mm, and the HDPE gasket almost has no deformation. As the displacement increases, the radius of the tunable lens become smaller and smaller. When the extrusive displacement gets larger, the maximum deformation is about 0.263 mm at 1 mm stroke. As the SEBS film is very thin, there is little impact on the results.

The Von Mises distributions of the lens static stress under different displacement loads are shown in Figure 5. It's not difficult to find that when the displacement becomes larger, the pressure increases gradually, and the maximum stress is 1.614 MPa which occurs in the top-right position of the inner HDPE gasket. When the displacement gets 1 mm, the maximum stress is 1.614 MPa which is much less than the yield strength of HDPE material (27 MPa), thus the safety factor of the structural strength meets the security requirement.

Rotating the simulation results around the axis Y, we can obtain the overall static deformation of the tunable lens under different displacement loads (Figure 6). The deformation of the intermediate part of the tunable lens is spherical approximately. As the displacement load increases, the radius of the sphere becomes smaller and smaller, which means that the focal length decreases and the lens focusing capability increases.

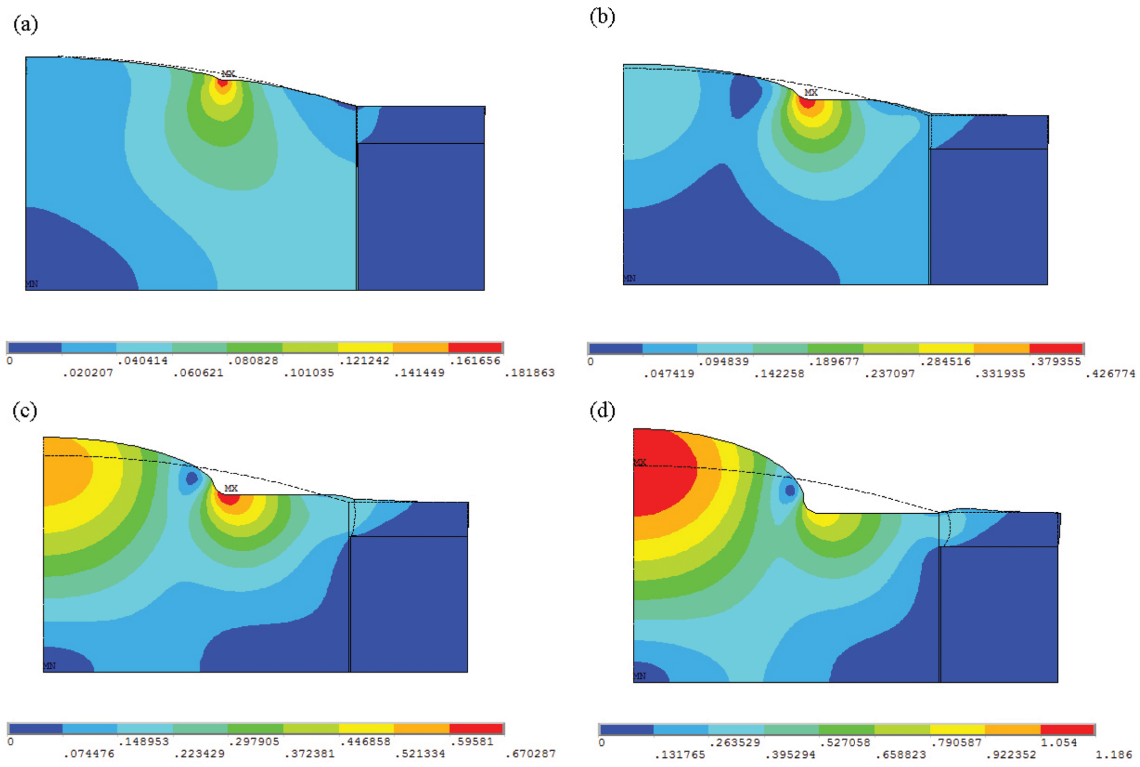

Figure 4. Deformation simulation of different displacement load: (a) 0.25 mm; (b) 0.5 mm; (c) 0.75 mm; (d) 1 mm.

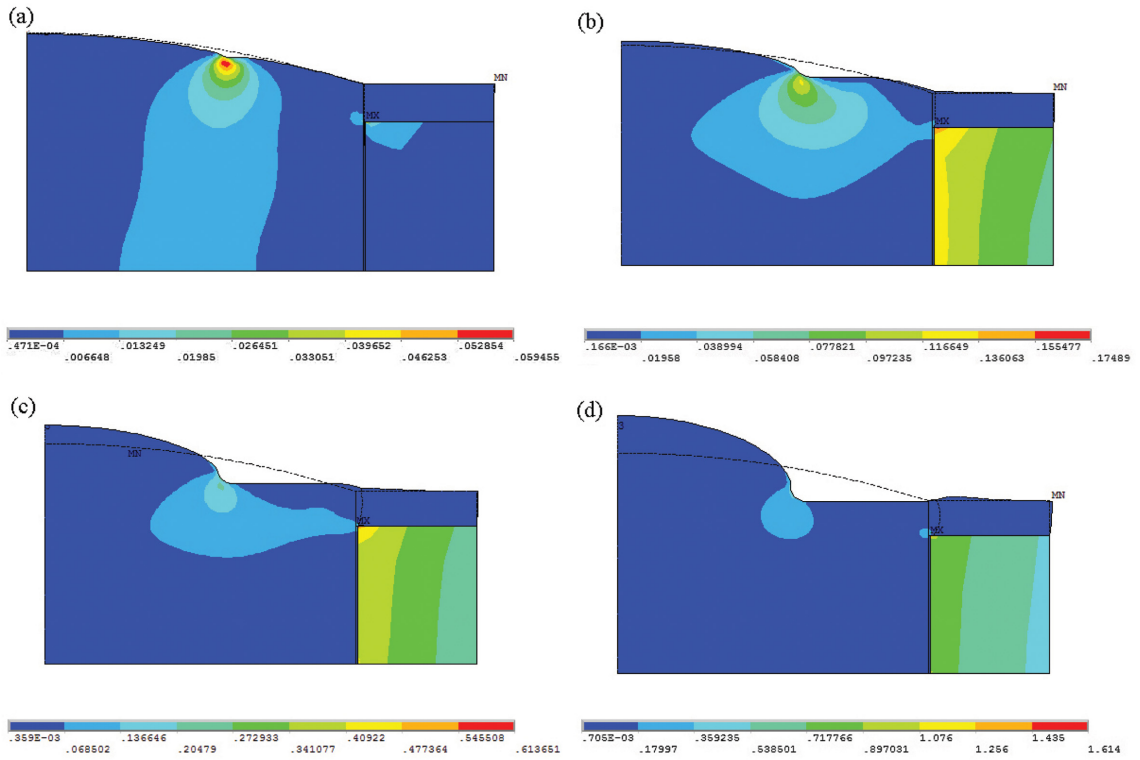

Figure 5. Static stress Von Mises distribution of the tunable-focus lens under different displacement load: (a) 0.25 mm; (b) 0.5 mm; (c) 0.75 mm; (d) 1 mm.

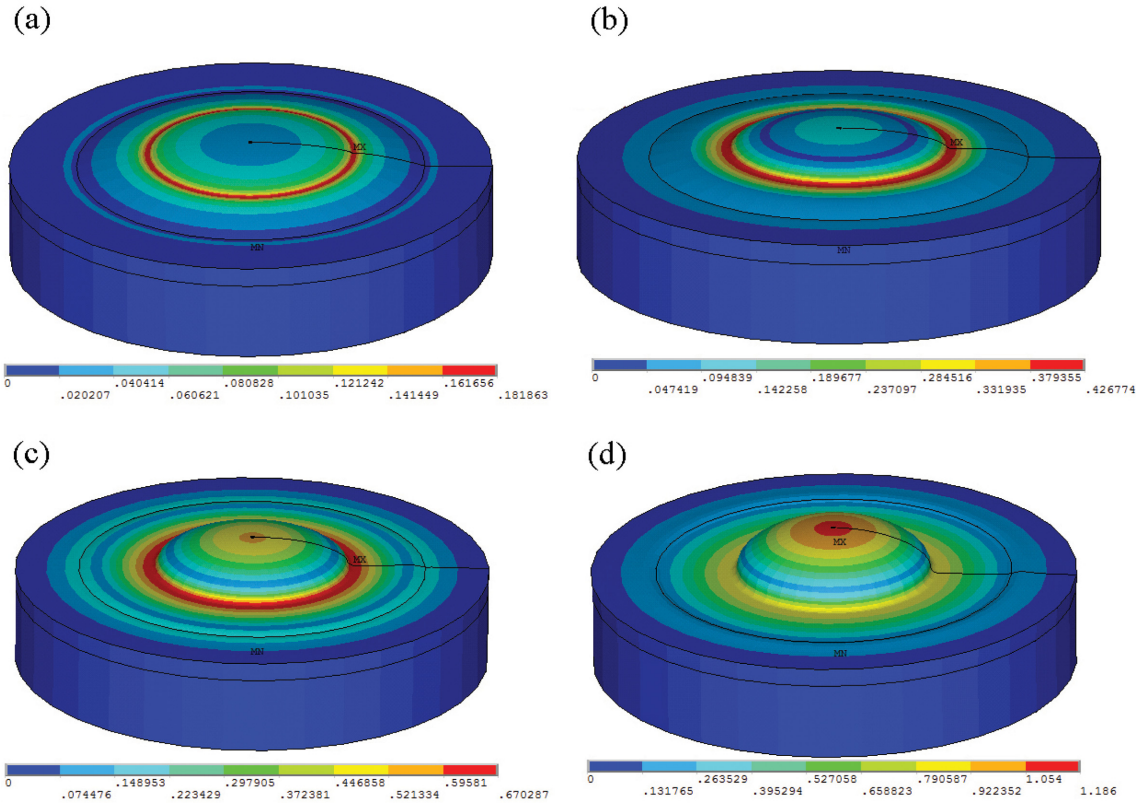

Figure 6. Overall deformation of the tunable lens under different displacement load: (a) 0.25 mm; (b) 0.5 mm; (c) 0.75 mm; (d) 1 mm.

Results and Discussion

To further analyze the imaging properties of the tunable-focus lens, we design and fabricate a set of experimental apparatus. The main components are as follows: a precise step motor, screw-and-nut mechanism, CCD chip, solid tunable lens (mentioned above), and the retaining ring. The prototype of this actuation device is shown in Figure 7. The rotation of the stepper motor makes the retaining ring squeeze the surface of the solid tunable lens through a screw-and-nut mechanism, causing the alteration of the lens curvature radius. By controlling the stepping angle (2 μm control accuracy), we can change the deformation of the solid tunable lens, thus altering the lens focal length.

To measure the surface profiles of the lens under different displacement loads, we use a non-contact three-dimensional scanner (OpticScan-D-Plus). The output displacement of the stepper motor is 0, 0.25, 0.5, 0.75 and 1 mm successively, and the data recorded is stored as IGS format. For each displacement, we choose the coordinates of 8 random points, and every point is in different position on the surface (mostly in the lower part). In order to facilitate the calculation, the vertex position is defined as the coordinate origin. By subtracting the vertex coordinates from the initial coordinates of the chosen points, we get the new coordinates $P(x, y, z)$. The spherical surface is described by

$$X^2+Y^2+(Z+R)^2=R^2 \tag{1}$$

Substituting the $P(x, y, z)$ of each point into eq. (1), a set of the spherical radius values corresponding to different displacement loads can be computed. Averaging the radius values of the same displacement loads, we can get the final value of the spherical radius R. In the solid tunable lens, the SEBS film can be analyzed as a concavo-convex lens. According to the general computation formula of focal length

$$f=\frac{f_1 f_2}{f_1+f_2}\to\infty \tag{2}$$

the SEBS film is equivalent to a parallel-plate glass. Therefore, the whole solid tunable lens can be approximated as a combination of two thin lenses: a PMMA lens and a PDMS lens.

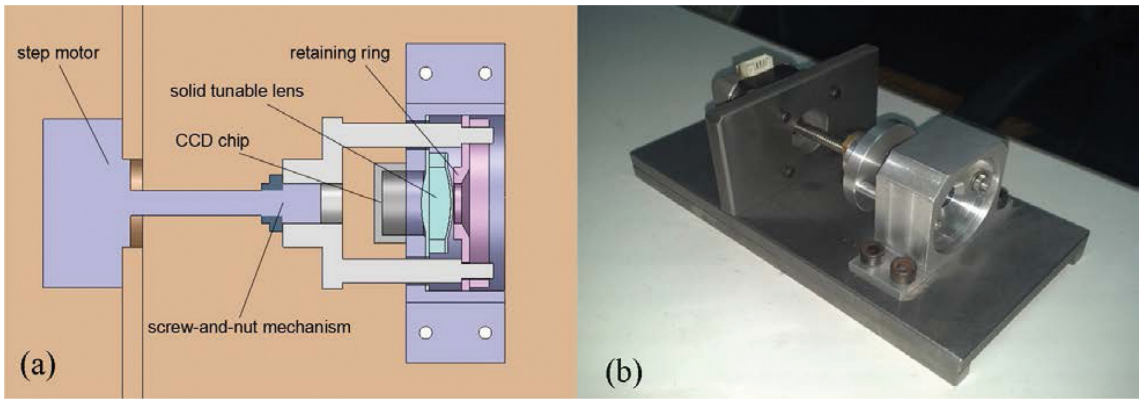

Figure 7. (a) Structure of the actuation device; (b) picture of the experimental device.

The focal length of the system can be calculated by

$$\Phi = \Phi_1 + \Phi_2 \tag{3}$$

where, $\Phi = 1/f$ is the focal power of the tunable lens, $\Phi_1 = 1/f_{PMMA}$, $\Phi_2 = 1/f_{PDMS}$. Considering the PMMA lens and the PDMS lens as two plano-convex lenses, the focal length can be given by

$$f_{PMMA} = \frac{R_{PMMA}}{n_{PMMA} - 1} \tag{4}$$

$$f_{PDMS} = \frac{R}{n_{PDMS} - 1} \tag{5}$$

According to the formula mentioned above and substituting the corresponding values, we can get the predicted focal length F_{pre} of the whole tunable lens under each displacement load.

Furthermore, to verify the reliability of the predicted focal length based on non-contact scanner measurement and assess the optical performance of the lens, the tunable device is connected to a computer. Adjust the step motor to control the displacements of the retaining ring, fix the tunable device, and translate a distant object along the lens axis until the sharpest image on the sensor plane is obtained, then the observed focal length can be approximated by measuring the distance between the CCD camera plane to the lens surface. The data of the spherical radius, predicted focal length, and observed focal length is shown in Table 1, and the captured images are shown in Figure 8.

Obviously, as the displacement ΔL increases, the spherical radius of the solid tunable lens decreases gradually. During the extrusion process, the curvature of the lens is smallest in the beginning, and gets bigger and bigger as the displacement increases. The agreement of the predicted and observed focal length is good, and the lens observed focal length changes from 31.8 to 14.1 mm. When the displacement load is smaller than 0.75 mm, we notice that the maximum deviation between

Table 1. Experimental Data of Displacement (ΔL), Lens Radius (R), Predicted Focal Length (F_{pre}), and Observed Focal Length (F_{obs})

ΔL (mm)	R (mm)	F_{pre} (mm)	F_{obs} (mm)
0	30.65	32.5	31.8
0.25	26.37	30.0	29.6
0.5	17.16	23.8	24.1
0.75	10.74	17.7	16.5
1	8.12	14.5	14.1

Figure 8. Images acquired under different displacement loads, from (a) to (d), the displacement load ΔL imposed to the lens surface is 0 mm, 0.5 mm, 0.75 mm, and 1 mm.

the predicted focal length and observed focal length is less than 0.7 mm. We change the displacement load from 0.75 to 1 mm at an interval of 0.05 mm, and notice that the average deviation value between the predicted focal length and observed focal length is 1.4 mm, which is much larger than the deviation value when displacement load is smaller than 0.75 mm. It might result from the irregular deformation under high displacement load, a larger deformation occurs in the periphery of the SEBS film, leading to part of PDMS deforming towards the lens edge, which would impact the lens optical stability and imaging quality. During the measurement process of the lens focal length and the imaging experiment, the displacement load is changed repeatedly, and the tunable lens shows good adjustability and quick response time. Qualitatively, images captured under all displacement loads are easily recognizable with a relatively low distortion. The image quality is better during the middle process of the extrusion than the beginning and the end stage. In the initial stage of compression, the lens inhomogeneity and asymmetry has great influence on imaging. With the increase of deformation, the lens high curvature would induce aberration and distortion. Keeping the homogeneity and structural symmetry during the lens fabrication process, optimizing the lens optical structure, surface curvature, thickness and aperture, and adopting new optical materials with high refractive index would be helpful to reduce the aberration and improve the optical properties of the polymer lens system. Placing the tunable lens with different inclination angle at different position, unlike the liquid lens, the solid tunable lens shows excellent resistance to the impact of gravity and vibration.

Conclusions

In this paper, we have developed a solid tunable lens made of polymer materials and analyzed its deformation and stress features through simulation and experiment. The lens focal length can be changed flexibly by altering the lens surface. A detailed description of the lens structure, materials and fabrication process is presented. The mechanical properties and deformation process are analyzed through finite element analysis. The relationships among the displacement, spherical radius, and focal length are measured and analyzed. The solid tunable lens is of simple controllability and quick response speed. The focal length can be reversibly transformed from 31.8 to 14.1 mm with good imaging quality. This paper offers a feasible way for the design, fabrication, and actuation of the solid tunable lens, which can be used in a variety of machine vision systems.

Acknowledgements: This research is supported by the National Natural Science Foundation of China (Project no. 51175459) and Science Fund for Creative Research Groups of National Natural Science Foundation of China (Project no. 51221004).

References

1. S. C. Park and W. S. Lee, *J. Korean Phys. Soc.*, **62**, 435 (2013).
2. S. Xu, Y. Liu, H. Ren, and S. T. Wu, *Opt. Express*, **18**, 12430 (2010).
3. S. Shian, R. M. Diebold, and D. R. Clarke, *Opt. Express*, **21**, 8669 (2013).
4. S. I. Son, D. Pugal, T. Hwang, H. R. Choi, J. C. Koo, Y. Lee, and J. D. Nam, *Appl. Opt.*, **51**, 2987 (2012).
5. G. H. Feng and Y. C. Chou, *Appl. Opt*., **48**, 3284 (2009).
6. N. Savidis, G. Peyman, N. Peyghambarian, and J. Schwiegerling, *Appl. Opt*., **52**, 2858 (2013).
7. L. Li and Q. H. Wang, *Opt. Eng*., **51**, 043001 (2012).
8. P. Brochu and Q. Pei, *Macromol. Rapid Commun.*, **31**, 10 (2010).
9. R. Marks, D. L. Mathine, G. Peyman, J. Schwiegerling, and N. Peyghambarian, *Opt. Lett*., **34**, 515 (2009).
10. S. Kuiper and B. H. W. Hendriks, *Appl. Phys. Lett*., **85**, 1128 (2004).
11. M. Blum, M. Büeler, C. Grätzel, and M. Aschwanden, *Proc. SPIE 8167*, 8167OW, Sep. 22, 2011. doi: 10.1117/12.897608.
12. N. Fraval, F. Berier, and O. Castany, *Proc. SPIE 8252*, 8252OQ, Feb. 9, 2012. doi: 10.1117/12.909233.
13. N. Fraval and J. L. D. B. de La Tocnaye, *Appl. Opt*., **49**, 2778 (2010).
14. Y. C. Tsai, P. K. Chung, W. P. Shih, and P. C. Su, *Microelectr. Eng*., **98**, 610 (2012).
15. G. Beadie, M. L. Sandrock, M. J. Wiggins, R. S. Lepkowicz, J. S. Shirk, M. Ponting, and E. Baer, *Opt. Express*, **16**, 11847 (2008).
16. E. J. Park, I. S. Kim, S. S. Park, H. S. Lee, and M. S. Lee, *Polym. Korea*, **37**, 744 (2013).
17. G. Wu, H. Zhang, and H. Zhang, *Polym. Korea*, **39**, 809 (2015).
18. J. W. Lee, J. H. Kim, S. G. Ji, K. S. Kim, and Y. C. Kim, *Polym. Korea*, **39**, 572 (2015).
19. S. H. Ra, H. D. Lee, and Y. H. Kim, *Polym. Korea*, **39**, 579 (2015).
20. S. H. Ra and Y. H. Kim, *Polym. Korea*, **38**, 602 (2014).
21. S. W. Bak, H. J. Kang, and D. W. Kang, *Polym. Korea*, **38**, 138 (2014).